

Lechosław Tuz, Krzysztof Sulikowski

Microstructure and Selected Mechanical Properties of Welded Joints in Austenitic Perforated Bottoms Made Using the Automated TOP TIG Method

Abstract: The article presents selected test results obtained during welding tests preceding a Welding Procedure Qualification, performed using a robotic TOP TIG welding station. The test results revealed the obtainment of welded joints characterised by proper geometry and proper austenitic structure. In addition, the article presents typical welding imperfections observed in relation to the adjustment of welding process parameters, i.e. hot cracks in the weld root area and cavities.

Keywords: perforated bottom, arc welding, austenitic steel

DOI: [10.17729/ebis.2019.2/7](https://doi.org/10.17729/ebis.2019.2/7)

Introduction

Heat exchangers are important system components in the refining, petrochemical and chemical industries as well as in industrial power engineering, heat engineering and gas engineering [1]. Extensive applications of heat exchangers necessitate the adjustment of their design to specific needs of both a given industrial sector and system. As a result, heat exchangers vary both in terms of their dimensions, the manner of assembly (i.e. one-way or multi-way systems) and materials they are made of (e.g. unalloyed steels, fine-grained steels, stainless steels, creep resisting steels, clad steel, aluminium alloys or nickel alloys) [1-5]. The design of heat exchangers and their materials are always adjusted to operating parameters, including the type, temperature, aggressiveness and the flow rate of media. [3-5]. However, in spite of design customisation, it is possible to differentiate between

various types of heat exchangers, e.g. heat exchangers with straight tubes and permanent perforated walls, with floating heads, U-shaped or helicoidal. The exchanger design includes an external jacket (external housing) and an internal part consisting of properly shaped tubes, barriers and perforated walls adjusting the flow of medium inside the exchanger.

The complexity of design as well as applied structural solutions significantly affect the service life of heat exchangers and their heat exchange efficiency. As a result, each “tailor-made” heat exchanger requires the adjustment of manufacturing processes to enable the obtainment of required product quality, including the satisfaction of gas directive requirements. As can be seen, the making of an appropriate product requires a number of operations, from the design and selection of materials, through production planning to the fabrication of a product

dr inż. Lechosław Tuz (PhD (DSc) Eng.) – AGH University of Science and Technology in Kraków;
mgr inż. Krzysztof Sulikowski (MSc Eng.) – Roboty Przemysłowe Sp. z o.o., Kraków

and its check. During production, because of laboriousness, the key stage is the making of girth welds in perforated walls connecting between tens and hundreds of tubes to a single bottom [6]. The foregoing results in the making of many repeatable welds in one product. Presently, the aforesaid welds are made by welders or using orbital welding machines, each time positioned by the operator.

The present market situation, characterised by the decreasing number of welders, an increase in welder's remuneration and the necessity of reducing the time of production are responsible for the fact that the welding of perforated walls should be performed using automatic welding stations. In turn, the necessity of satisfying specific customer's requirements necessitates the use of automatic welding machines based on welding robots enabling the quick adjustment of the process both in relation to the tube and the bottom material as well as to the geometry of the perforated bottom itself. In addition to primary functionalities of a welding robot, the above-named welding station should enable fast retooling and adjustment to a material being welded, often involving the changes of a welding method, e.g. the MAG method applied when welding unalloyed steels and the TIG method used when welding stainless steels and nickel alloys. The changeable geometry and dimensions of perforated walls and tubes as well as the arrangement of the latter in the perforated bottom indicate that a crucial element of the welding station is an autonomous system detecting edges to be welded and, at the same time, controlling the position of the robot arm, significantly reducing time needed for the programming of the welding. In addition, in cases of materials sensitive to a heat input, it is possible to optimise the welding sequence in order to avoid the distortion (deformation) of a perforated bottom and the formation of undesirable structures (e.g. martensite) or inclusions (e.g. carbides on grain boundaries, sigma phases etc.). Steels sensitive to a heat input include austenitic steel grades such as 304 or

316. In addition, when welding the above-named steels it is recommended to use a filler metal in order to reduce welding stresses and to prevent the formation of hot cracks in the weld.

The article presents selected test results obtained when developing a technology enabling the welding of perforated bottoms made of austenitic stainless steel grade 316/316L with DN 20 tubes having a wall thickness of 1 mm. The welding process was performed using a robotic welding station of Roboty Przemysłowe Sp. z o.o., composed of a ArcMate 120iC12L welding robot (Fanuc) integrated with a Nertamatic 450 welding power source (Lincoln Electric) for TOP TIG welding (featuring automated filler metal wire feeding) and an iRVision video system (FANUC) detecting edges to be welded. Figure 1 presents a photograph of a fragment of a welding torch with a visible gas nozzle, a tungsten electrode and a filler metal wire feeding system. The research work aimed to develop a preproduction technology enabling the welding of perforated bottoms made of austenitic steels, performed using the TIG method and the filler metal. The tests led to the development of a preliminary welding procedure specification (pWPS) and the making of a welded joint in accordance with EN ISO 15614-8 for the purpose related to the welding procedure qualification.

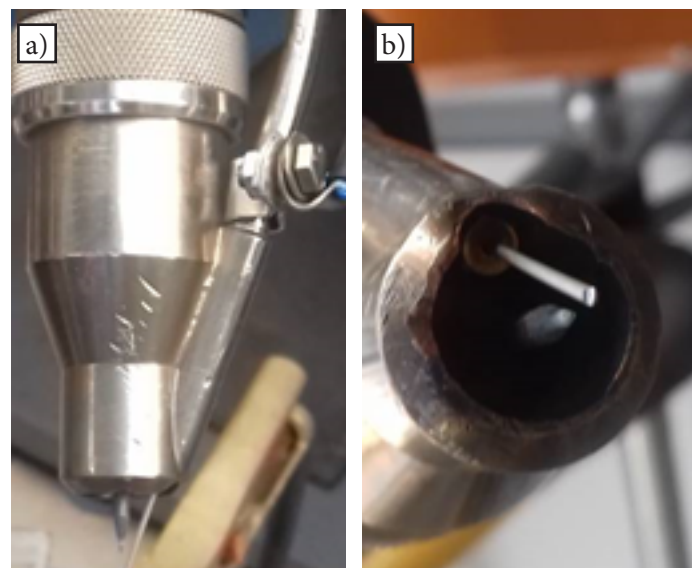


Fig. 1. Gas nozzle with the filler metal feeder (a) and the position of the filler metal wire in relation to the pointed electrode tip (b)

Test material

The test specimen was a joint made of a 20 mm thick plate containing drilled openings having a diameter of 24 mm. The distances between axes of the openings amounted to 34 mm. The openings were located interchangeably and the arrangement of the tubes was triangular. The edges of the openings were bevelled ($1/45^\circ$). Tubes having an external diameter of 24 mm and a wall thickness of 1.5 mm were placed in the openings. To improve the matching of the tubes to the opening surface, the tubes were subjected to mechanical bulging. During the welding process, the perforated plate was positioned vertically, enforcing welding in the vertical down and vertical up positions when making the girth welds. The welding process was completed at the top of the tube. The above-named manner of welding required changing the welding torch position and the distance between the electrode of the welded material during the individual stages of the process. Figure 1

presents the gas nozzle featuring the feeding of the filler metal, whereas Figure 2 presents the pre-weld preparation of edges and the characteristic dimensions of the welded joint. The welding process resulted in the obtainment of a girth joint with the butt weld (BW). The welding process involved the making of two welds. The first run was made without, whereas the second run was made with the filler metal. The key criteria used when assessing the quality of the process included (1) the lack of welding imperfections (including cracks), the gentle toe angle between the weld and the material of the tube and of the perforated bottom (without undercuts) and the lack of overlap as well as (2) the automated making of successive girth welds, i.e. the detection of edges to be welded and the welding process itself.

The perforated test plate was made of steel 316, whereas the tube was made of steel 316L. The filler metal used in the tests was a wire made of steel grade 316, having a diameter of

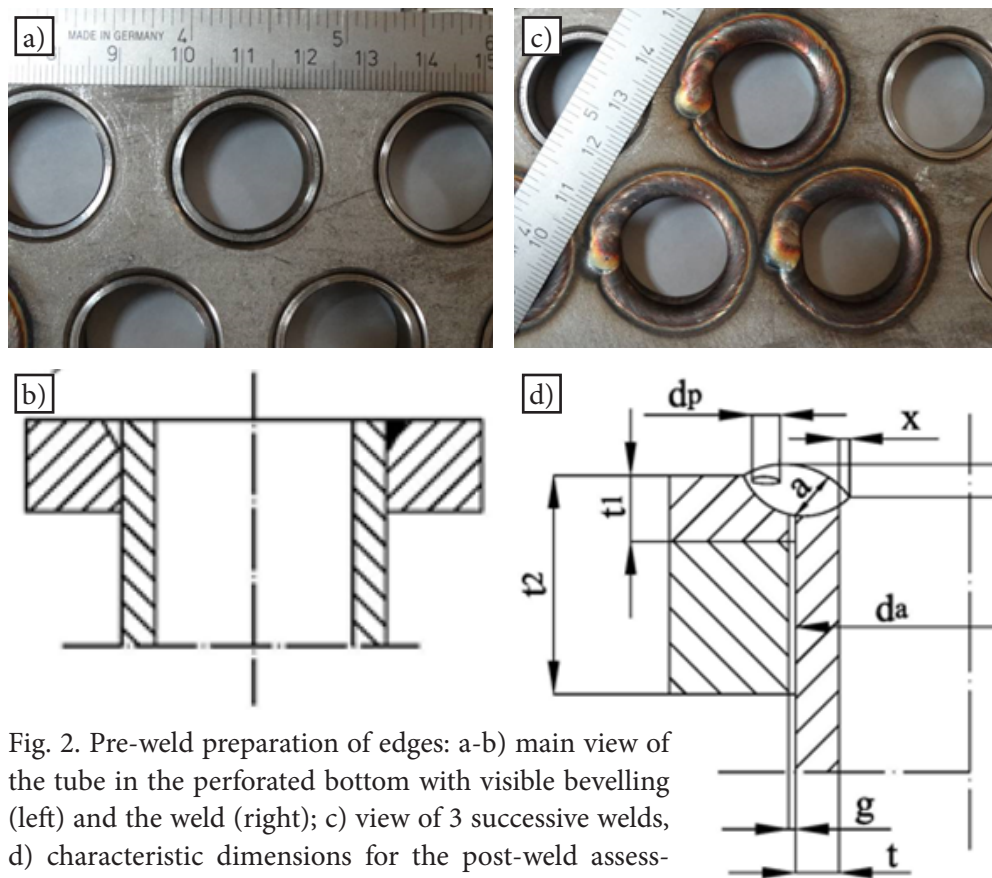


Fig. 2. Pre-weld preparation of edges: a-b) main view of the tube in the perforated bottom with visible beveling (left) and the weld (right); c) view of 3 successive welds, d) characteristic dimensions for the post-weld assessment of the weld shape: t_1 – thickness of plated coating (if any), t_2 – thickness of the perforated plate, t – thickness of the tube, d_a – internal diameter of the tube, g – gap between the tube and the perforated plate, a – weld thickness, d_p – gas pore size, x – overlap

1 mm. As can be seen, all of the materials used in the tests belonged to the same material group (1.4401/1.4404, 8.1 in accordance with ISO 15608). The chemical compositions of the steels used to make the welded joint are presented in Table 1. The shielding gas used during welding was argon (I1 in accordance with EN ISO 14175).

The joints were subjected to visual, penetrant and non-destructive tests including macro and microscopic examinations performed using a light microscope as well as cross-sectional Vickers test-based hardness

measurements (HV₅) of the welded joint. Specimens used in microscopic tests were subjected to mechanical grinding involving the use of water abrasive paper and to polishing involving the use of polishing cloth and the aqueous slurry of Al₂O₃. The above-presented metallographic specimens were subjected to electrolytic etching in the 10% alcoholic solution of chromium oxide (VI).

Visual and macroscopic tests

Visual tests revealed an even weld face around the entire circumference, without visible scaliness. The area marking the termination of the welding process revealed a gentle transition of the crater into the welding process commencement area (calm arc termination). The tests did not reveal any porosity in the weld area or cracks in the crater. The lack of cracks was confirmed by penetrant tests. Macroscopic tests performed in cross-section along the axis of the tube revealed proper penetration and properly shaped welds, i.e. the lack of overlap, gentle transition into the tube material and the slightly convex face. The macroscopic tests did not reveal the presence of cracks. The gap between the tube and the surface of the perforated bottom opening was nearly non-existent (proper matching of surfaces as a result of the upsetting of the tube end). The macroscopic observations of the weld revealed that the penetration of the second run included the metal of the first run. The thickness of the weld did not exceed 2 mm. Figure 3a presents a weld with two visible runs, whereas Figure 3b presents a joint with a welded overlap. In turn, Figure 4 presents macrostructures

Table 1. Chemical composition of steel 316/316L in accordance with EN 10088, % by weight

EN 10088	X5CrNiMo17-12-2 (1.4401)	X2CrNiMo17-12-2 (1.4404)
AISI USA	316	316L
C	<0.07	<0.03
Si	<1.0	<1.0
Mn	<2.0	<2.0
P	<0.045	<0.045
S	<0.015	<0.015
N	<0.11	<0.11
Cr	16.5-18.5	16.5-18.5
Mo	2.0-2.5	2.0-2.5
Ni	10.0-13.0	10.0-13.0

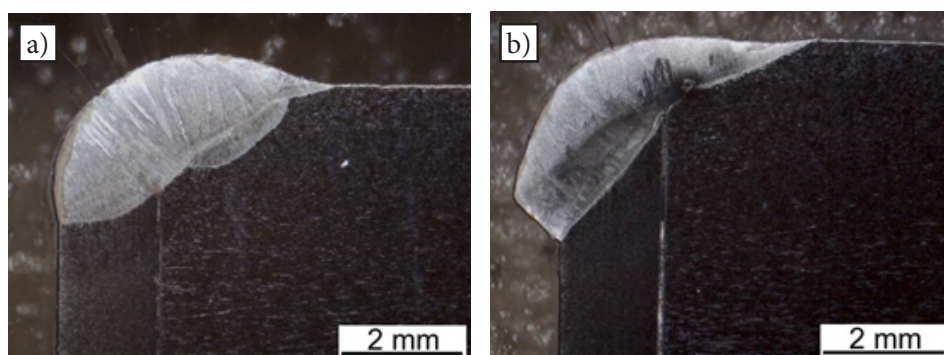


Fig. 3. Macrostructure of welded joints: a) multi-run structure, b) weld overlap (improper shape); the joints were subjected to microscopic examinations

of 3 successive welded joints made in the automatic welding mode. The obtained welds were characterised by high repeatability.

Microscopic tests

In order to identify the structure and internal welding imperfections (if any), when adjusting welding process parameters, radiographic tests were replaced with microscopic tests. The tests involved metallographic specimens subjected to grinding, polishing and electrolytic etching. Figure 5a presents the proper weld with clearly visible run no. 1, made without the filler metal, and run no. 2, made using the filler metal (joint macrostructure in Fig. 3a). The weld structure was dendritic, with the lattice of ferrite δ (Fig. 5b and 5c). The HAZ area was characterised by the slight grain growth and the presence of ferrite δ bands (Fig. 5d). The base material of the perforated bottom and the tube contained the austenitic structure with a slight amount

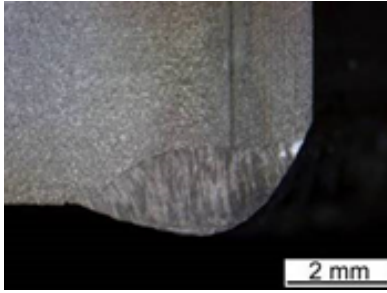
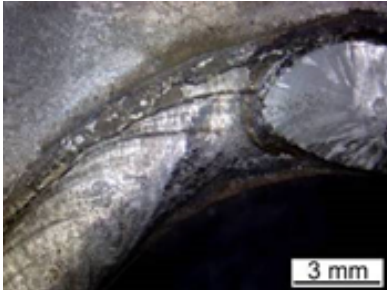
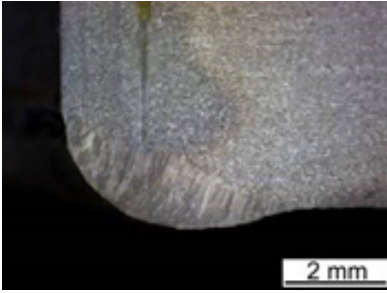
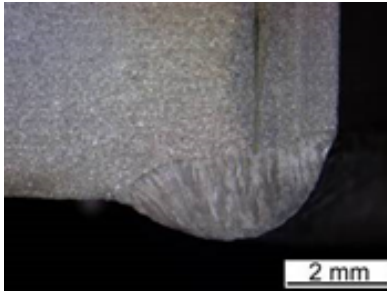
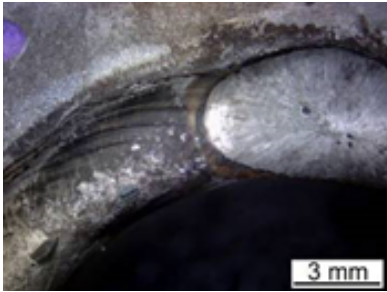
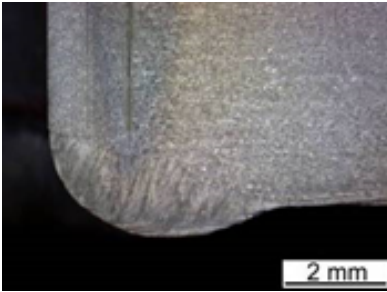
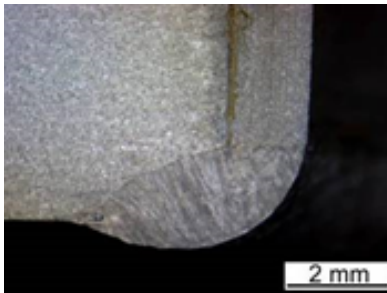
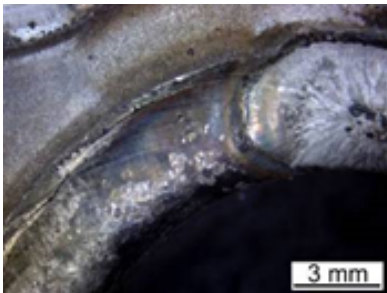
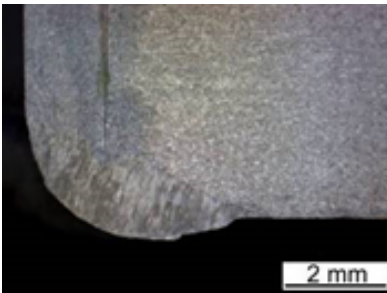
Joint number	Left side of the girth weld in cross-section	Weld face with visible welding termination area	Right side of the girth weld in cross-section
4			
5			
6			

Fig. 4. Macrostructure of girth welded joints made in the automated welding mode

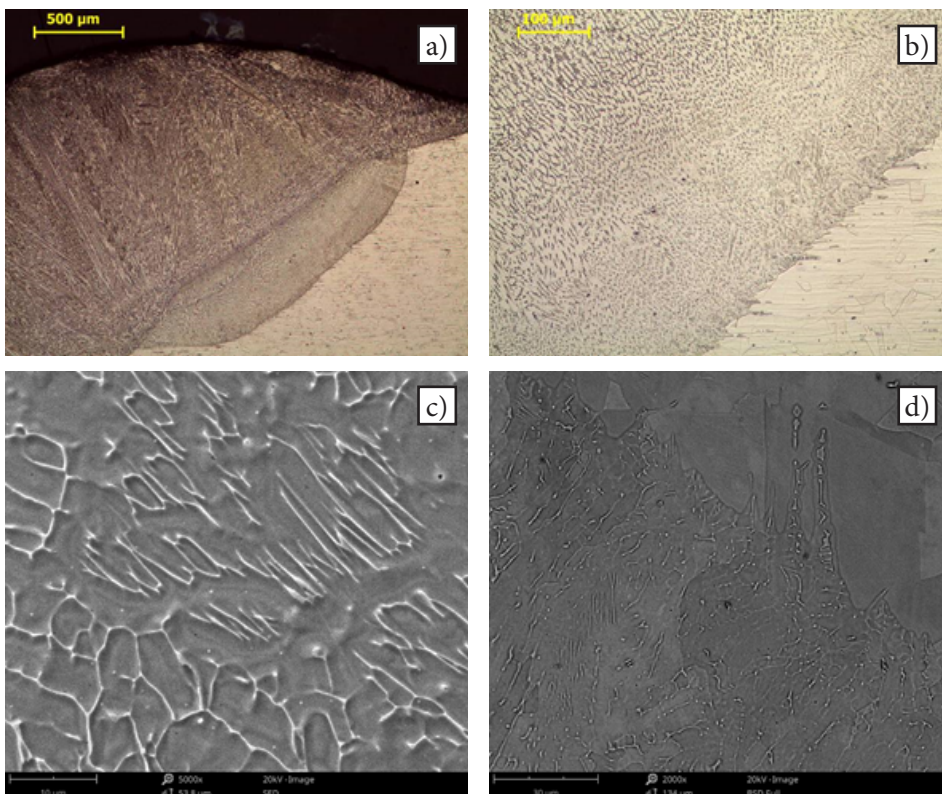


Fig. 5. Microstructure of the proper welded joint: a) main view of the weld with visible runs, b) weld structure with the visible lattice of ferrite δ , c) weld structure and d) structure near the fusion line with the visible band of ferrite δ

of ferrite δ in the chemical composition segregation bands. The structure of the base material contained twin boundaries.

Microscopic observations revealed the presence of gas cavities located primarily near the fusion line (Fig. 6b). Gas cavities were characteristic of the welded joints, where the electric arc of the first run was moved on the external edge of the tube, quickly melting the edge and reducing the length of the tube. The above-named operation of the arc also led to the formation of an overlap (Fig. 6a), the height of which reached up to 1 mm. The welding process performed

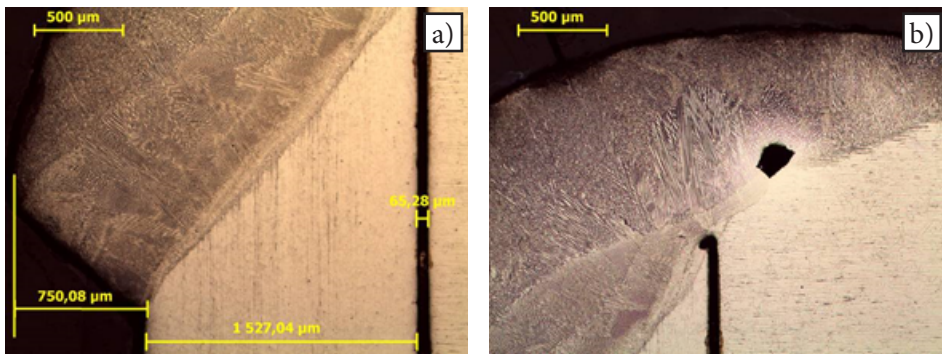


Fig. 6. Welded joint: a) with the overlap and characteristic geometric dimensions, b) gas cavity in the area between the runs near the fusion line

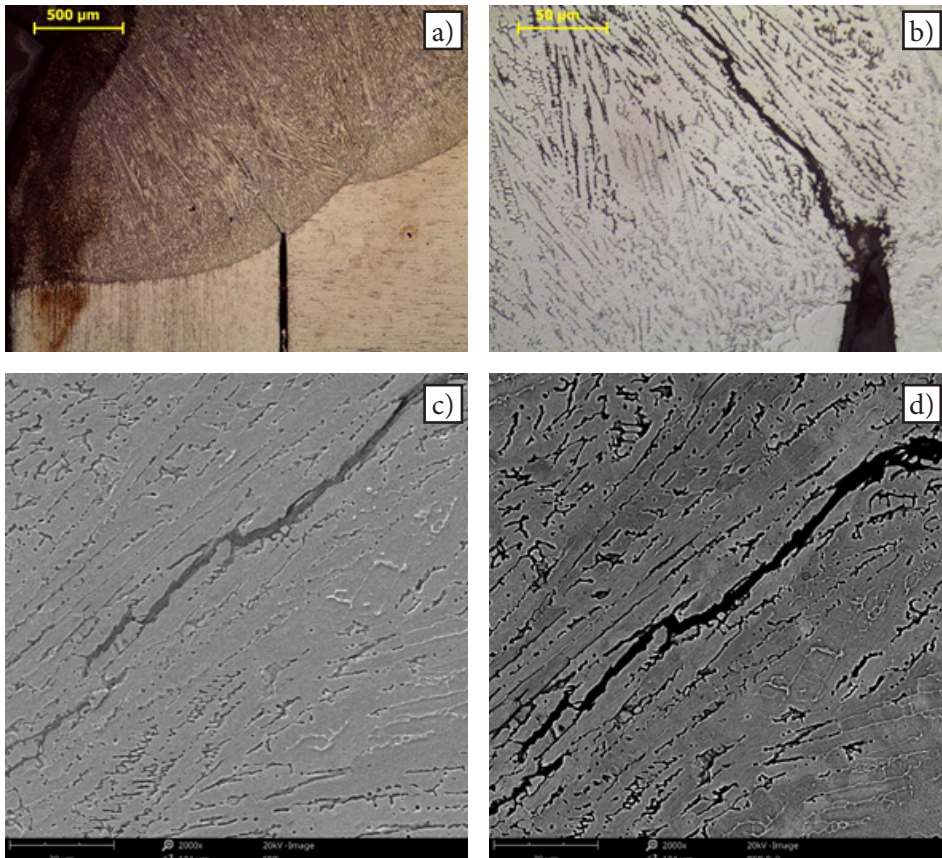


Fig. 7. Hot crack in the weld root area initiated from the gap: a) main view, b) crack and porosity near the crack, (light microscopy) c-d) crack and porosity (SEM image)

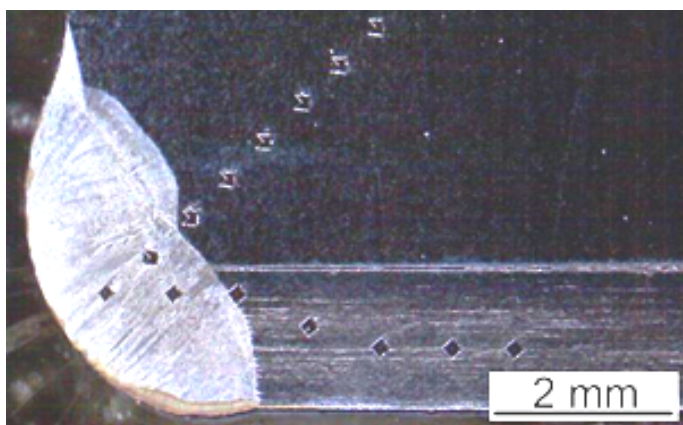


Fig. 8. Hardness measurement area in the cross-section of the welded joint

using overly low current parameters led to the formation of hot cracks and porosity located near the cracks, which is typical of austenitic steels characterised by a relatively wide high-temperature brittleness range. During cooling, when the amount of dendrites in the liquid increased, interdendritic areas began to lack liquid metal, which led to the formation of discontinuities. In turn, because of contraction and an increase in tensile stresses in the weld, bridges formed between dendrite branches were incapable of transferring tensile stresses, which led to the formation of cracks (Fig. 7) [7]. The foregoing necessitated the proper making of the first run. The first run was made without the filler metal. Arc heat melted the edge of the perforated bottom material and the metal of the tube (reducing its length). The molten metal formed the weld (characterised by relatively small volume) and preheated the perforated bottom. The second run, made using the filler metal, filled the depletion of the tube length, and led to the formation of the slightly convex weld face. Because of their location and small size, the revealed cracks and porosity were undetectable in radiographic tests.

Hardness measurements

Hardness measurements based on the Vickers hardness test were performed in cross-section, along two measurement lines, using an indenter load of 5 kG for 10 seconds. Figure 8 presents

Table 2. HV5 hardness measurement results (measurement lines in accordance with Figure 8)

Area	Weld		HAZ	Base material				
	1	2		3	4	5	6	7
Horizontal (tube)	207	189	181	196	190	182	185	-
Oblique (perforated bottom)	-	187	179	195	186	184	174	176

the arrangement of indents in the cross-section of the joint, whereas Table 2 presents measurement results. The measured values were restricted within the range of approximately 175 HV₅ to approximately 210 HV₅, i.e. values typical of welded joints made in austenitic steels. The weld and the HAZ revealed a slight increase in hardness in comparison with that of the base material.

Summary and conclusions

The tests involving the welding of perforated bottoms, performed using the robotic TOP TIG process, revealed the possibility of satisfying the requirements of the EN ISO 15614-8 standard as regards the automated welding of austenitic perforated bottoms. However, to prevent the formation of hot cracks in the weld root area it is necessary to precisely adjust process parameters. Because of their location and shape, the above-named hot cracks are impossible to detect through radiographic tests. In addition, because of the specimen preparation manner and relatively low magnification values applied, hot cracks may remain undetected during macroscopic tests. An additional test applicable during the welding procedure qualification related to perforated bottoms is a squeeze test, enabling the identification of cracks (if any). However, the aforesaid test requires particular attention, where any doubts should be verified using scanning electron microscopy (fractographic tests).

An issue following the proper adjustment of welding process parameters is the identification of the location of individual welded joints. To this end, it is recommended to use edge detecting video systems, enabling the quick identification of the entire edge along with its position in relation to the perforated bottom. The system integrated with the robot arm enables the autonomous

correction of the arm movement trajectory and repeatable detection of welded joints.

The obtained joints were characterised by the following features:

- repeatable shape of the weld and the uniform, slightly convex face,
- lack of weld overlaps, surface cracks and cracks on the weld root side,
- austenitic structure of the weld with the ferrite δ lattice in interdendritic areas,
- uniform distribution of hardness and the narrow heat affected zone.

References

- [1] Kakac S., Liu H., Pramuanjaroenkij A.: Heat Exchangers, Selection, Rating, and Thermal Design, CRC Press, 2012.
- [2] Pokrzywniak C., Kulawski L.: Wymienniki ciepła. Gaz, 2008, no. 5, pp. 26-34.
- [3] Szulc P., Tietze T., Rączka P., Wójs K.: Porównanie wybranych konstrukcji wymienników ciepła pracujących w układzie odzysku ciepła odpadowego ze spalin wylotowych. Archiwum Energetyki, 2013, vol. XLIII, no. 1-2, pp. 11-30.
- [4] Mukherjee R.: Effectively Design Shell-and-Tube Heat Exchangers. Chemical Engineering Progress, 1998, vol. 94, no. 2.
- [5] Spencer D., Leggoe J., Hu X., Fuller G., Godfrey D., Assuring the Integrity of Air-cooled Heat Exchanger Tube to Tubesheet Welds. CEED Seminar Proceedings, 2009, pp. 7-12.
- [6] Adamiec P., Adamiec J.: Niezawodność spoin gwarancją jakości urządzeń energetycznych. Archiwum Odlewnictwa, 2006, no. 6.
- [7] Tasak E.: Metalurgia spawania. Wydawnictwo Jak, Kraków, 2008.